

Supporting information

S1. Relation between the pressure jump across the particle-laden interface and the surface pressure of absorbed monolayer.

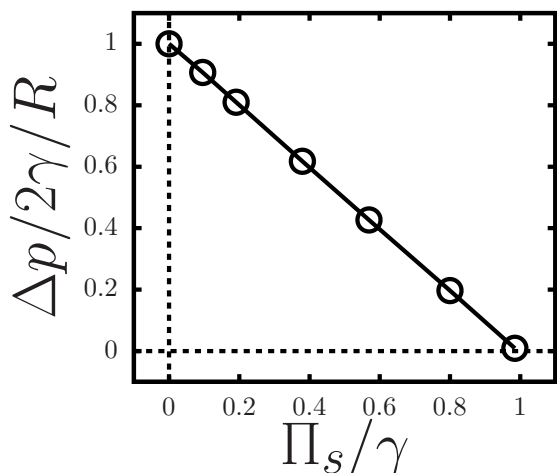


Figure 1 Symbols: the normalized pressure difference between the inside and outside of a spherical drop versus the normalized surface pressure as computed from the simulation. Continuous line: equation $\Delta p/(2\gamma/R) = 1 - \Pi_s/\gamma$.

To make sure FIPI yields the correct pressure field across the fluid interface, an initial spherical drop is gradually compressed by an attached particle monolayer. The pressure difference between inside and outside of the drop is explicitly calculated from simulations. The results are compared with Young-Laplace equation incorporated with surface pressure. The simulations done by FIPI accurately capture the real pressure difference under different surface pressure created by the particle monolayer.

S2. Proof of independence of surface pressure on particle size for a linear inter-particle force relation.

For a hexagonal array, the relation between the average inter-particle separation and ϕ_s is

$$l = \left(\frac{2\sqrt{3}\pi a^2}{3\phi_s} \right)^{1/2}. \quad (1)$$

Assuming nearest neighbour interactions within hexagonal packing, the packing energy can be estimated as

$$\begin{aligned} E_p &\approx N_c N \langle F_{pi} \rangle l \\ &= N_c \frac{4\pi R^2 \phi_s}{\pi a^2} \langle F_{pi} \rangle \left(\frac{2\sqrt{3}\pi a^2}{3\phi_s} \right)^{1/2} \\ &= N_c \frac{12R^2 \phi_s}{a} \left(\frac{2\sqrt{3}\pi}{3\phi_s} \right)^{1/2} \langle F_{pi} \rangle. \end{aligned} \quad (2)$$

The coordination number N_c is independent of a . Therefore $\Pi_s \approx \frac{E_p}{2A} \propto \phi_s^{1/2} \langle F_{pi} \rangle / a$, which proves that Π_s is approximately independent of a when $\langle F_{pi} \rangle \propto a$ for fixed ϕ_s . The linear inter-particle force model (4) employed in this paper enjoys this property as it allows to investigate the effects caused by changing only the particle size.

S3. Convergence of buckling time with decreasing s

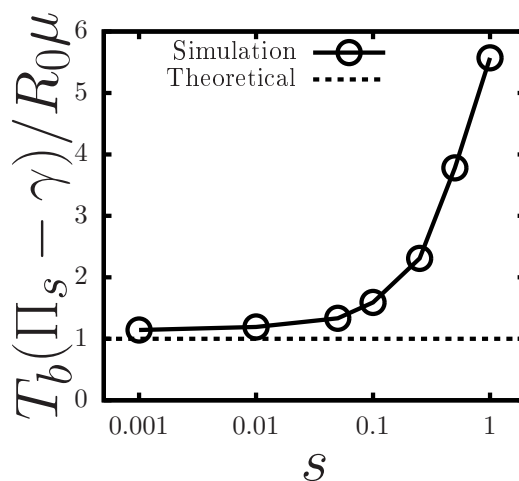


Figure 2 Normalised buckling time vs. nondimensional diffusion length s for $f = 10.0$ and $\Pi_s/\gamma = 1.71$. The dashed line is the value calculated according to equation (8).

The parameter $s = \frac{\sqrt{M\mu}}{\epsilon}$ defines the magnitude of the diffusion of phase field variable with respect to a certain fluid interface thickness. It is necessary that s has to be large enough to keep the thickness of fluid interface as constant. On the other hand, for fluid interface with finite thickness, any finite value of s will damp the fluid velocity around fluid interface to some extent. As a result the fluid interface takes longer to buckle as s increases, which is shown in Figure 2. The convergence of buckling time is achieved by decreasing s to 0 while keeping the fluid interface thickness ϵ as constant.

S3. Equivalence between increasing spring constant k at fixed liquid volume and decreasing liquid volume at fixed spring constant k

In our simulation, changing the volume of the drop at fixed spring constant k or increasing k for fixed liquid volume leads, qualitatively, to the same results. The reason for this behaviour is that the pressure in an incompressible fluid is a Lagrange multiplier that depends - for a given value of the energy associated to the particle-covered interface - only on the volume of the fluid comprised within the interface. In other words, the value of the pressure across the interface adjusts itself to the drop volume and the configuration of the particle monolayer with respect to the fluid interface, regardless of whether the drop volume is reduced by keeping the monolayer fixed, or the monolayer area is artificially “expanded” by keeping the volume fixed and increasing the surface pressure.

Figure 3 shows snapshots from two simulations. In one simulation (Fig. 3 TOP), the volume of the drop is kept fixed and the surface pressure increased by increasing k . In the other, the spring constant is kept constant and the volume of the drop slowly decreased in a quasi-static manner. The essential geometric features of the two buckled morphologies are the same in the two figures. We do not expect, of course, to obtain identical morphologies, as the buckling instability is highly sensitive to the exact configura-

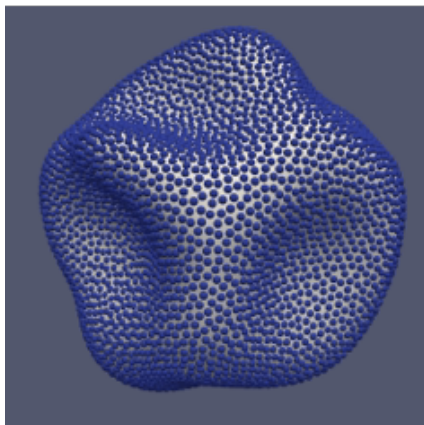
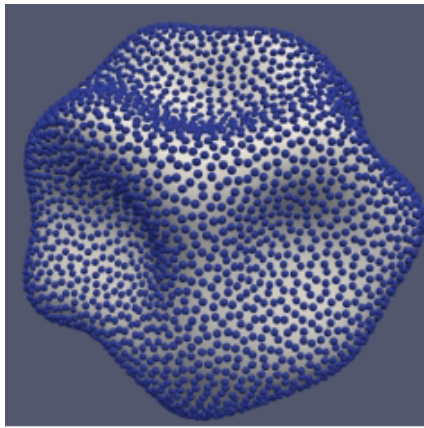


Figure 3 Buckled morphology for (TOP) the case in which the spring constant k is increased and the volume of the drop is kept constant and (BOTTOM) for the case in which the spring constant is kept fixed and the drop volume is reduced.

tion of each particle.